

Antiplasmodial Activity of Green-Synthesized MgO Nanoparticles Using *Achillea* millefolium Against Chloroquine-Resistant and-Sensitive *Plasmodium falciparum*

Niloufar Khamsehpour¹, Haleh Hanifian¹, Mehdi Nateghpour^{1,2*}, Ahmad Raeisi^{1*}, Mohammad Shabani³, Gholamreza Hassanpour⁴, Aram Khezri¹, Seyed Ahmad Dehdast⁴, Leila Farivar¹ and Saeed Shahsavari⁵

- 1. Department of Medical Parasitology and Mycology, School of Public Health, Tehran University of Medical Sciences, Tehran, Iran
- 2. Research Center for Quran, Hadith and Medicine, Tehran University of Medical Sciences, Tehran, Iran
- 3. Department of Biochemistry, School of Medicine, Iran University of Medical Sciences, Tehran, Iran
- 4. Center for Research Endemic Parasites of Iran, Tehran University of Medical Sciences, Tehran, Iran
- 5. Department of Biostatistics and Epidemiology, School of Health, Alborz University of Medical Sciences, Karaj, Iran

* Corresponding authors: Mehdi Nateghpour, Ph.D., Department of Medical Parasitology and Mycology, School of Public Health, Tehran University of Medical Sciences,

Tehran, Iran

Ahmad Raeisi, Ph.D.,
Department of Medical
Parasitology and Mycology,
School of Public Health, Tehran
University of Medical Sciences,
Tehran, Iran
Tel: +98 9123278020
E-mail:
nateghpourm@sina.tums.ac.ir,
raeisia@tums.ac.ir

Received: 16 Feb 2025 Accepted: 30 Aug 2025

Abstract

Background: Resistance to antimalarial medications, particularly in *Plasmodium falci-parum* (*P. falciparum*), has emerged as a significant challenge, highlighting the need for innovative therapeutic strategies. Green-synthesized magnesium oxide nanoparticles (MgO NPs) represent a promising approach to therapeutic interventions. This study presents one of the first detailed evaluations of green-synthesized MgO NPs derived from *Achillea millefolium* (*A. millefolium*) against both chloroquine-sensitive (3D7) and chloroquine-resistant (K1) *P. falciparum* strains.

Methods: In this study, MgO NPs were biosynthesized using *A. millefolium* extracts with varying solvent ratios. The nanoparticles were characterized using UV-Vis, FTIR, FESEM, and DLS techniques. Cytotoxicity was assessed *via* MTT and hemolysis assays. Their antiplasmodial efficacy was evaluated *in vitro* against chloroquine-sensitive (3D7) and -resistant (K1) *P. falciparum* strains.

Results: The synthesized MgO NPs displayed quasi-spherical morphology and nanoscale size. Among tested formulations, the most effective showed IC₅₀ values of 0.17 *mg/ml* for the 3D7 strain and 0.76 *mg/ml* for the K1 strain, indicating significant antiplasmodial activity.

Conclusion: Green-synthesized MgO NPs using *A. millefolium* demonstrated potent antiplasmodial activity at low IC₅₀ concentrations, showing efficacy against both chloroquine-sensitive and -resistant *P. falciparum* strains. These findings highlight their promise as plant-based nanotherapeutics for malaria treatment.

Keywords: Achillea millefolium, Antimalarials, Chloroquine, Magnesium oxide, Malaria, Plasmodium falciparum

To cite this article: Khamsehpour N, Hanifian H, Nateghpour M, Raeisi A, Shabani M, Hasanpour Ghr, *et al.* Antiplasmodial Activity of Green-Synthesized MgO Nanoparticles Using *Achillea mille-folium* Against Chloroquine-Resistant and-Sensitive *Plasmodium falciparum*. Avicenna J Med Biotech 2025;17(4):249-257.

Introduction

Malaria remains one of the leading causes of mortality worldwide; however, prompt detection and timely intervention can prevent severe outcomes ¹. The treatment of malaria is becoming increasingly challenging due to the emergence of drug-resistant *Plasmodium falciparum* (*P. falciparum*) strains, which exhibit resistance to nearly all currently available antimalarial agents. This poses a critical obstacle to effective disease management. Although chemotherapy has histori-

cally played a pivotal role in malaria control, its efficacy is now undermined by rising treatment failures, underscoring the urgent need for novel therapeutic strategies ². Medicinal plants continue to serve as a valuable source of bioactive compounds with antimalarial potential, offering benefits such as reduced toxicity, cost-effectiveness, and physiological compatibility. However, their clinical application is often limited by poor solubility, low bioavailability, and *in vivo* instability.



Recent advances in nanotechnology have opened promising avenues for overcoming these limitations by enabling the development of nano-based drug delivery systems that enhance the pharmacological properties of plant-derived compounds ³. Achillea millefolium L., a medicinal herb rich in flavonoids, phenolic acids, and terpenes, has demonstrated antimicrobial, antioxidant, and anti-inflammatory activities ⁴. Although it has shown potential in managing parasitic and infectious diseases, its application against malaria has not yet been thoroughly investigated ^{5,6}.

In the present study, a novel green synthesis approach was introduced for the fabrication of magnesium oxide nanoparticles (MgO NPs) using aqueous and ethanol extracts of *Achillea millefolium* (*A. millefolium*). To the best of our knowledge, this is the first report utilizing *A. millefolium* for MgO NP synthesis with an emphasis on antiplasmodial evaluation. This phytochemical-assisted method offers several advantages: it is conducted at 80°C temperature and pressure, does not require chemical catalysts or thermal annealing, and utilizes the plant extract as a natural chelating and reducing agent, ensuring an eco-friendly and energy-efficient process.

Previous studies have highlighted the antimicrobial and antiparasitic properties of MgO NPs synthesized through various green and chemical routes, particularly against bacterial and fungal pathogens. However, their antiparasitic potential, especially against *Plasmodium* spp., remains underexplored. This study addresses this gap by evaluating the biological activity of synthesized MgO NPs using *A. millefolium*, with a specific focus on their antimalarial effects.

Materials and Methods

Plant extraction

The extraction of *A. millefolium* was conducted at Iran University of Medical Sciences. Dried flowers were separated from roots, ground into fine powder, and 1 *g* of the powder was mixed with 100 *ml* of solvent in varying ratios of Distilled Water (DW) and 96% ethanol (EtOH): 50:50, 70:30, and 30:70 (DW: EtOH). Each mixture was stirred at 200 *rpm* using a magnetic stirrer and subjected to reflux extraction at 70°*C* for 3 *hr*. The mixtures were then cooled to room temperature and filtered using Whatman No. 1 filter paper.

Biosynthesis of MgO NPs

 physicochemical characterization and bio-logical evaluation.

Characterization

MgO NPs were characterized using UV-visible spectroscopy (UV-2450, PerkinElmer), Fourier-trans-form infrared spectroscopy (FTIR; Tensor 27, Bruker, Germany), field emission scanning electron microscopy (FESEM; TESCAN MIRA3, Czech Republic), dynamic light scattering (DLS; HORIBA SZ-100), and zeta potential analysis (HORIBA SZ-100). The UV-visible spectrum was recorded from 200-800 nm. FTIR analysis was used to identify functional groups involved in nanoparticle synthesis. FESEM assessed surface morphology, while DLS and zeta potential provided information on size distribution and colloidal stability, respectively.

Hemolysis assay

Hemolytic activity of the *A. millefolium* extracts and MgO NPs was evaluated on human erythrocytes using a spectrophotometric method. Fresh heparinized O⁺ blood was washed thrice with Phosphate-Buffered Saline (PBS, ph=7.0) and suspended in normal saline to a concentration of 1%. A stock solution (total volume $1000\,\mu l$) was prepared by combining $660\,\mu g/ml$ of extract or MgO NPs with $340\,\mu g/ml$ of normal saline. Serial dilutions (0.125, 0.25, 0.5, and $1\,mg/ml$) were prepared and mixed with erythrocyte suspensions. After $1\,hr$ of incubation at $37\,^{\circ}C$, samples were centrifuged and the absorbance of the supernatant measured at $541\,nm$. Hemolysis percentage was calculated as:

% hemolysis =
$$\frac{Hb_{ABS}}{Hb_{Hb_{100}\,\%\,ABS}} \times 100$$

Cultivation of P. falciparum and preparing complete culture medium (CCM)

P. falciparum strains 3D7 and K1 were cultured using the Trager and Jensen method with modifications. The Complete Culture Medium (CCM) consisted of RPMI-1640 supplemented with HEPES, 50 *mg/L* hypoxanthine, 50 *mg/L* gentamicin, and Human AB+se-rum. Infected blood samples (two drops) were added to 4.5 *ml* CCM. Non-infected erythrocytes were prepared by washing whole blood three times with saline, centrifuged at 5000 *rpm* for 5 *min*, and used to adjust hematocrit to 10%. Cultures were maintained at 37°C in a humidified incubator with 5% CO₂, 5% O₂, and 90% N₂. Subculturing occurred every 48 *hr* until parasitemia reached 2% (K1) or 3% (3D7).

MTT assay

Cytotoxicity of synthesized MgO NPs (from 30:70 and 50:50 DW: EtOH extracts) was assessed on Human Dermal Fibroblasts (HDF) *via* MTT assay. HDF cells were cultured in DMEM-High Glucose medium (Biowest, USA) supplemented with penicillin/ streptomycin (Gibco, USA) at 37°C with 5% CO₂. After trypsinization and neutralization, cells were seeded in 96-well plates. MTT reagent (Sigma-Aldrich, USA) was

added and incubated for 3 hr. After removing the medium, $100 \mu l$ of DMSO (Bioldea, Iran) was added to dissolve formazan crystals. Absorbance was read at 570-630 nm (BioTek, USA). Cell viability was calculated as:

Cell survival rate =

Optical absorption in the experimental group
Optical absorption in the control group × 100

In vitro antiplasmodial assay

Stock solutions of MgO NPs derived from A. millefolium extracts were prepared in RPMI medium at concentrations of 0.125, 0.25, 0.5, and 1 mg/ml. Chloroquine was used as a standard reference drug, formulated in the same medium at concentrations of 1, 5, 25, and 50 µg/ml. Additionally, MgCl₂ was assessed in RPMI at equivalent concentrations of 0.125, 0.25, 0.5, and 1 mg/ml. Each stock solution was utilized to prepare serial dilutions of MgO NPs in a 96-well microplate, with positive control wells containing RPMI with infected Red Blood Cells (iRBCs) and negative control wells containing RPMI with uninfected RBCs. All assays were conducted in triplicate, with 20 μl of infected RBCs added to each well. Following a 24-hr incubation period at 37°C, parasitemia levels were assessed using Giemsa staining methodology. This staining technique is essential for visualizing the presence of parasites within the erythrocytes. The effectiveness of the various extracts was quantitatively evaluated by calculating the average percentage suppression of parasitemia, employing the following formula:

Statistical analysis

Data analysis was conducted using GraphPad Prism, employing two-way ANOVA for statistical testing.

Significance levels were indicated as follows: * for p< 0.05, ** for p<0.01, *** for p<0.001, and **** for p< 0.0001.

Results

Characterization of MgO Nps by UV-VIS Spectroscopy

To confirm the successful synthesis of MgO NPs, UV–Vis spectroscopy was performed to evaluate their optical properties. As shown in figure 1, absorbance measurements were recorded across the 200-800 *nm* range, which aligns with previously published studies on MgO NPs ⁸. The spectrum exhibited a prominent absorption peak between 250 *nm* and 300 *nm*, characteristic of MgO NPs synthesized *via* green methods using *A. millefolium* extract. This finding corroborates earlier studies and confirms nanoparticle formation.

Fourier transform infrared spectroscopy (FTIR)

The FTIR analysis was performed to identify the functional groups of bioactive molecules in the A. millefolium extract involved in reduction, capping, and stabilization of MgO NPs. Figure 2 illustrates spectral differences between the plant extracts and the synthesized MgO NPs. The broad peak observed between 3200-3400 cm⁻¹ corresponds to O-H stretching vibrations of hydroxyl groups present in phenols and alcohols. The peak at 2979 cm⁻¹ is related to asymmetric and symmetric C-H stretching vibrations of methyl groups. A peak at 1642 cm⁻¹ indicates C=C stretching characteristic of alkenes, while bands at 1384 cm⁻¹ correspond to C-H bending or O–H bending in phenolic compounds. Peaks in the range of 1080–1043 cm⁻¹ indicate C–O stretching vibrations typical for alcohols and ethers. Importantly, the peak between 450–750 cm⁻¹ confirms metal–oxygen (Mg-O) bond formation, verifying the successful synthesis of MgO NPs 9.

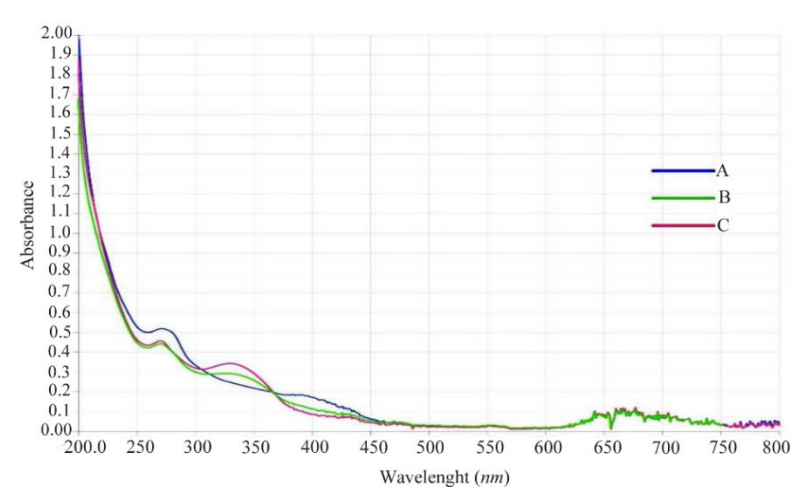


Figure 1. Ultraviolet-visible (UV-Vis) spectroscopy of green-synthesized MgO nanoparticles using the plant extract of *Achillea millefolium*, in three different proportions.

A) 30D.W:70ETH, B) 50D.W:50ETH, and C) 70D.W:30ETH.

Antiplasmodial Activity of Green-Synthesized MgO NPs

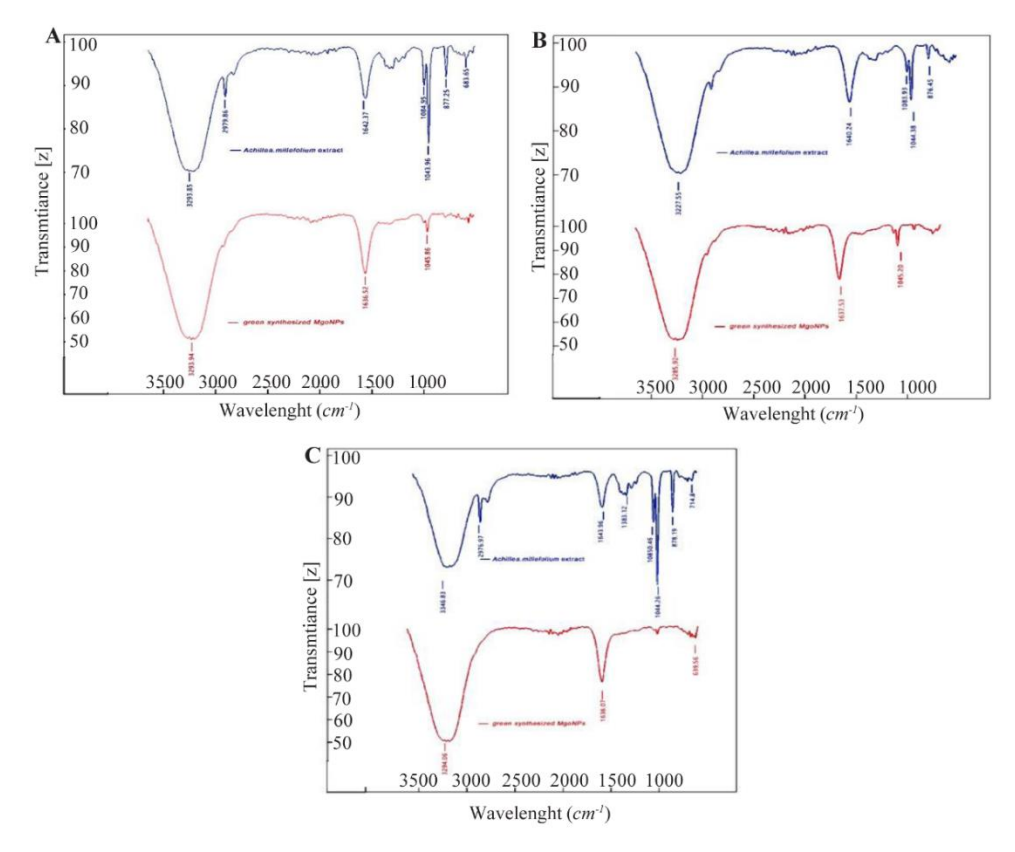


Figure 2. FTIR spectrum of three different proportions of *A. millefolium* extracts and synthesized MgO nanoparticles. A) 30D.W:70ETH, B) 50D.W:50ETH and C) 70D.W:30ETH.

Field Emission Scanning Electron microscopy (FE-SEM)

The morphology and size of the sample were examined using Scanning Electron Microscopy, as illustrated in figure 3. Analysis of the obtained images reveals that the synthesized MgO NPs exhibit a size range of 20 nm to 60 nm (with a mean size of approximately 40 nm). Furthermore, the green-synthesized MgO NPs appear quasi-spherical and tend to form agglomerates, likely attributable to the interactions and van der Waals forces present among the particles ^{9,10}.

Particle size and surface analysis of MgO NPs

Dynamic Light Scattering (DLS) analysis showed that the hydrodynamic diameters of MgO NPs varied depending on the extraction solvent ratio: 126.2 nm for 30:70 DW: EtOH, 161 nm for 50:50 DW: EtOH, and 356.9 nm for 70:30 DW: EtOH formulations (Figure 4). The presence of a single sharp peak in each case suggests a relatively homogeneous particle size distribution. Zeta potential measurements revealed low surface charges of $-2.2 \, mV$, $+12.3 \, mV$, and $-2.3 \, mV$ for the three formulations, respectively (Figure 5). These relatively low zeta potential values indicate moderate colloidal stability, as values above $\pm 30 \, mV$ are typically required for good electrostatic stabilization in suspension.

Hemolysis assay on human erythrocytes

The hemolytic activity of both *A. millefolium* extracts and MgO NPs was quantified (Figure 6). The results

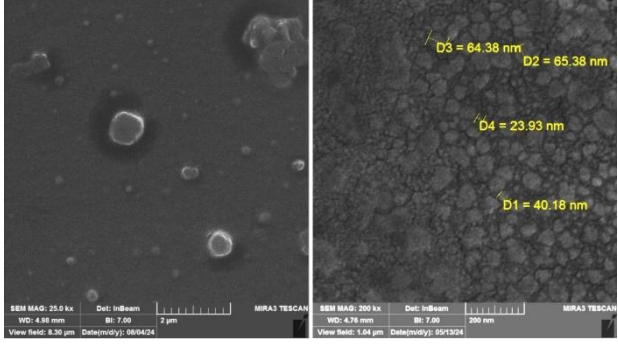


Figure 3. Fe SEM images of MgO nanoparticle.

show that MgO NPs caused significantly less hemolysis compared to the crude plant extracts, suggesting better hemocompatibility of the synthesized nanoparticles.

MTT assay

The MTT assay was conducted to evaluate the cytotoxicity of MgO NPs on HDF cells. Concentrations tested ranged from 0.125 to 1 mg/ml. As shown in fig-

Khamsehpour N, et al

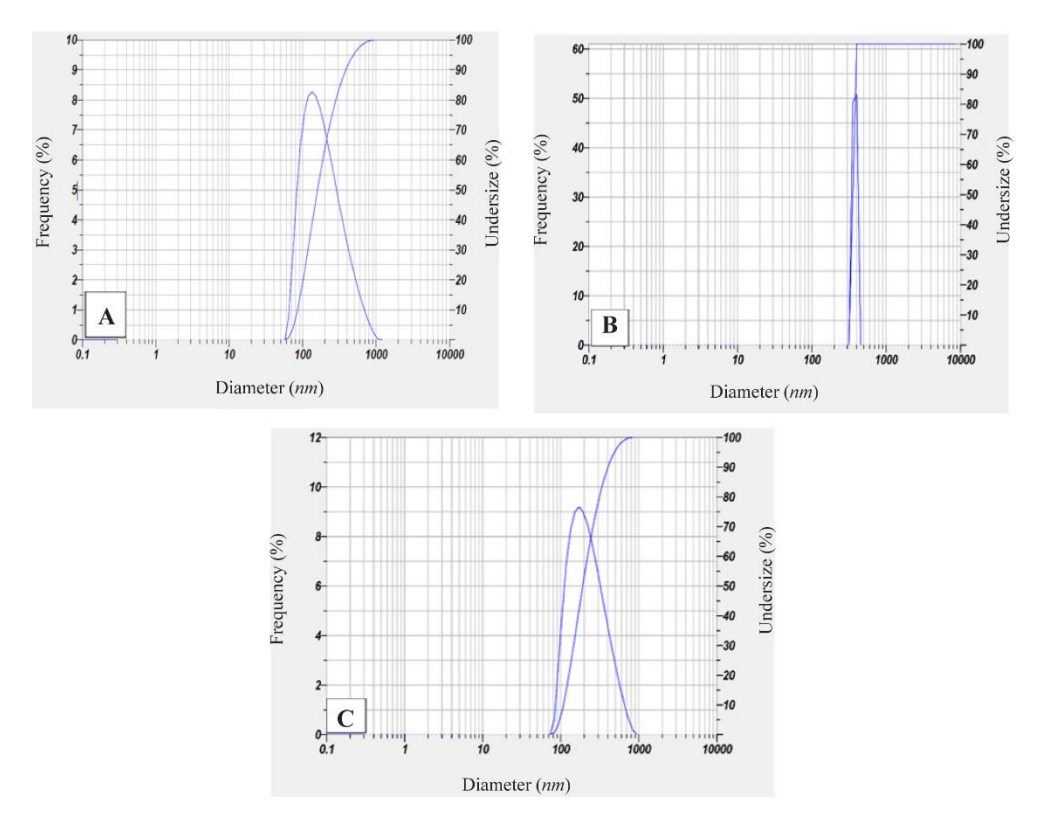


Figure 4. Histogram of size distribution from the dynamic light scattering (DLS) analysis of biosynthesized *Achillea millefolium* MgO NPs at three different proportions. A) 30D.W:70ETH, B) 50D.W:50ETH, and C) 70D.W:30ETH.

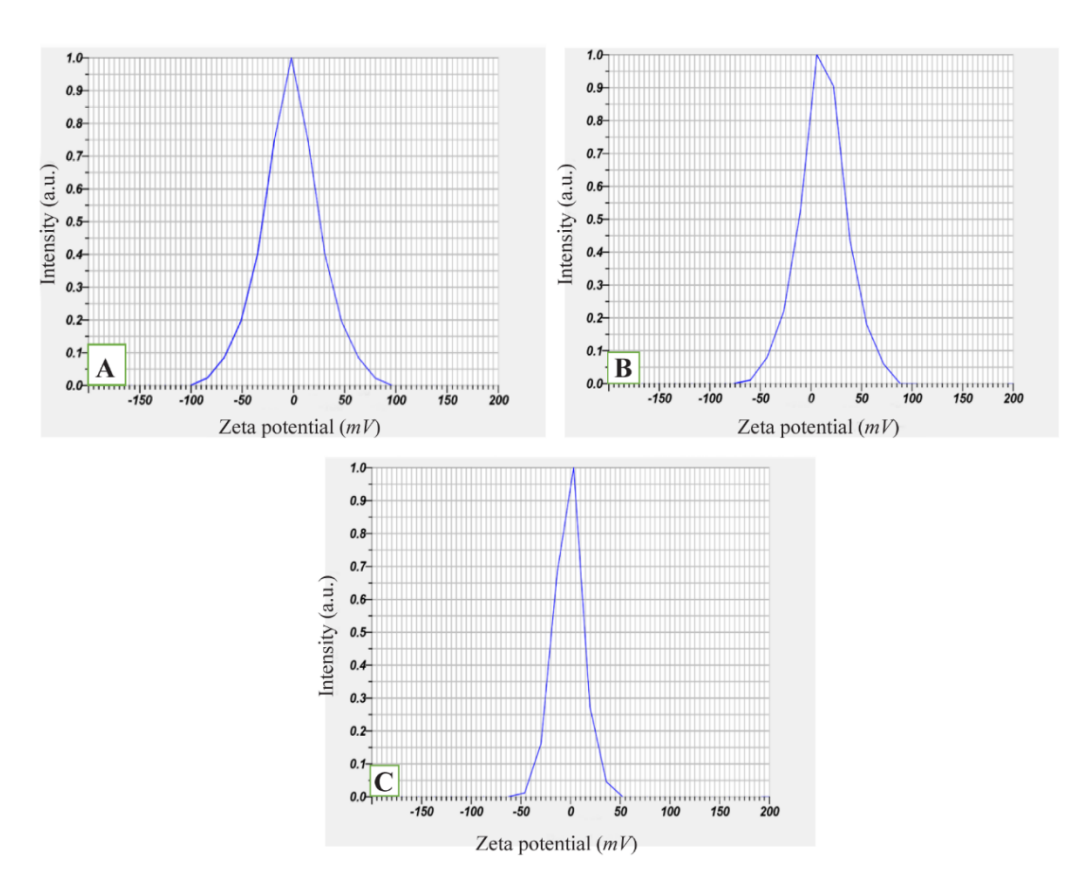


Figure 5. Zeta potential of Achillea millefolium MgO NPs. The value zeta potential of A.millefolium MgO NPs with three different proportions. A) 30D.W:70ETH, B) 50D.W:50ETH, and C) 70D.W:30ETH.

Antiplasmodial Activity of Green-Synthesized MgO NPs

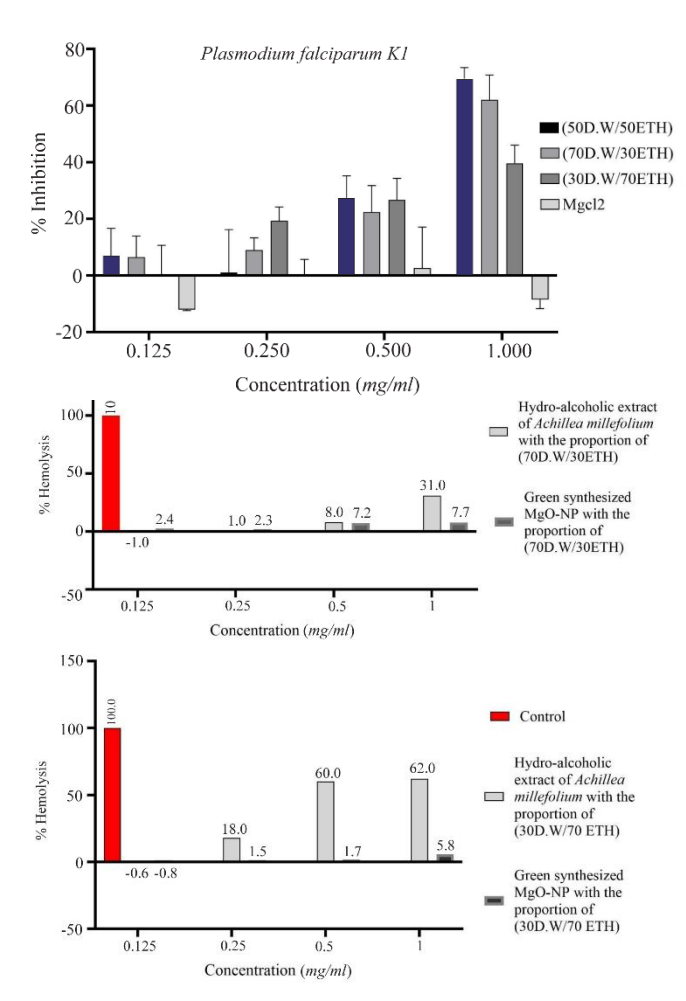


Figure 6. Inhibition percent of RBC hemolysis by *Achillea mille-folium* extract *and A. millefolium* MgO NPs.

ure 7, a dose-dependent decrease in cell viability was observed, with MgO NPs synthesized using the 30:70 DW: EtOH formulation exhibiting lower cytotoxicity than the 50:50 formulation. Statistical significance was assessed *via* two-way ANOVA, and error bars represent the standard deviation of triplicate experiments.

Anti-plasmodial effects of synthesized MgO NPs

The antiplasmodial activity of MgO NPs was evaluated against chloroquine-sensitive (*P. falciparum* 3D7) and chloroquine-resistant (*P. falciparum* K1) strains. The IC₅₀ values against 3D7 were 0.25 *mg/ml* for 50:50 DW: EtOH, 0.38 *mg/ml* for 70:30 DW: EtOH, and 0.17 *mg/ml* for 30:70 DW: EtOH formulations. Against the resistant K1 strain, IC₅₀ values were higher: 0.76 *mg/ml*, 0.84 *mg/ml*, and 1.04 *mg/ml*, respectively. For com-

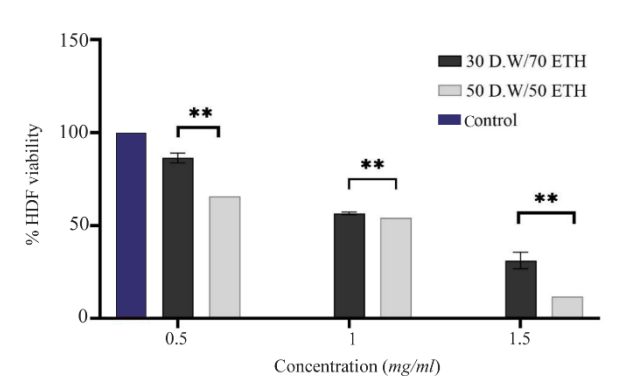


Figure 7. the MTT assay of MgO NPs with proportions of (30D.W:70ETH) and (50D.W:50ETH) at three different concentrations: 0.5 mg/ml, 1 mg/ml, and 1.5 mg/ml. The results of the Tukey multiple comparisons test indicate a statistically significant finding, at **p<0.01.

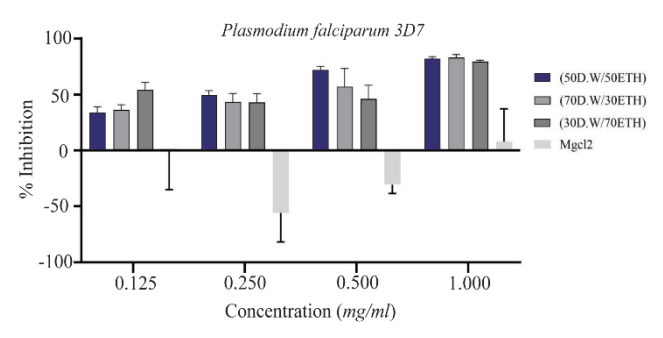


Figure 8. The growth-inhibitory effect of MgO NPs at three different proportions: (30 D.W:70 ETH), (50D.W:50 ETH), and (70 D.W:30 ETH), based on the *Plasmodium falciparum* strain 3D7 and MgCl2. Two-way ANOVA showed differences between proportions are not significant.

parison, chloroquine's IC₅₀ values were 0.17 *mg/ml* (3D7) and 7.35 *mg/ml* (K1). The 30:70 DW: EtOH formulation demonstrated the most potent antiplasmodial activity, comparable to chloroquine against the sensitive strain (Table 1, Figures 8 and 9). This enhanced activity may relate to increased extraction of bioactive compounds with ethanol-rich solvent, contributing to better nanoparticle efficacy.

Discussion

Malaria remains a significant global health challenge, especially in tropical and subtropical regions. This is largely driven by the increasing emergence of drug-resistant *P. falciparum* strains. Despite progress in vector control and antimalarial treatments, the limited availability of new therapeutic agents calls for alternative

Table 1. Determination of MgO NPs and chloroquine IC50 on P. falciparum species

Ratio	MgONPs P. falclparum 3D7	MgONPs P. falclparum K1	Chloroquine P. falclparum 3D7	Chloroquine P. falclparum K1
30:70 DW:EtOH	$0.17 \ mg/ml$	1.04~mg/ml		
50:50 DW:EtOH	0.25~mg/ml	$0.76 \ mg/ml$	$0.17 \mu g/ml$	$7.35 \mu g/ml$
70:30 DW:EtOH	0.38 mg/ml	$0.84\ mg/ml$		

strategies. In this study, the successful green synthesis of MgO NPs using aqueous and ethanol extracts of *A. millefolium*, a medicinal plant known for its antimicrobial and antiparasitic properties was reported. This environmentally friendly and cost-effective synthesis approach is scalable and offers promising potential for sustainable nanomedicine development ¹¹⁻¹⁶.

UV-Vis spectrophotometric analysis revealed a prominent absorption peak between 250 and 300 *nm* (Figure 1), consistent with previously reported biologically synthesized MgO NPs ^{17,18}. This absorption confirms the formation of MgO NPs and their characteristic

Figure 9. The growth-inhibitory effect of MgO NPs at three different proportions: (30D.W:70ETH), (50D.W:50ETH), and (70D.W: 30ETH), based on the *Plasmodium falciparum* strain K1 and MgCl2. Two-way ANOVA showed differences between proportions are not significant.

nanoscale optical properties. FTIR spectra (Figure 2) identified functional groups including hydroxyl, carbonyl, and ether bonds, suggesting that phenolic compounds and flavonoids in *A. millefolium* play key roles in the reduction and stabilization of Mg²⁺ ions during synthesis. These findings align with previous reports where phytochemicals from medicinal plants such as *Ocimum sanctum* and *Azadirachta indica* facilitated nanoparticle biosynthesis ¹⁹⁻²¹.

FESEM analysis provided direct visualization of the nanoparticle morphology, revealing quasi-spherical MgO NPs with diameters ranging from 20 to 60 nm (Figure 3). This morphology aligns with previous reports of spherical MgO NPs synthesized using plants such as *Clitoria ternatea* and *Emblica officinalis*, which exhibited particle sizes between 25 and 60 nm ¹⁴. Such nanoscale dimensions are known to enhance cel-lular penetration and interaction with biological targets due to their high surface area-to-volume ratios.

DLS analysis revealed a size distribution ranging from 126.2 to 356.9 nm, depending on the ethanol: water ratio used in extraction (Figure 4). The discrepancy between DLS and SEM data is expected due to hydrodynamic diameter inclusion and aggregation in solution, as previously reported by Gatou et al ²². Zeta potential analysis showed that only the 50:50 DW: EtOH formulation exhibited moderate colloidal stability (12.3 mV), while the other two had low surface charges (-2.2 and -2.3 mV) (Figure 5). These results indicate that nanoparticle formulations are sensitive to extraction solvent polarity, which may affect not only physical stability but also biological interactions.

Hemocompatibility testing revealed that MgO NPs induced significantly lower hemolysis compared to the crude A. millefolium extract (Figure 6), suggesting that nanoparticle formulation may reduce the toxicity of bioactive plant compounds when administered systemically. This observation is important when considering therapeutic applications in humans. In addition, MTT cytotoxicity assays conducted on HDF cells indicated a

dose-dependent reduction in cell viability, with the (30:70) ethanol: water formulation being the least cytotoxic (Figure 7). The lower cytotoxicity may be associated with differences in phytochemical content and resulting particle characteristics such as size and surface charge. Similar findings were reported in previous studies, where green-synthesized MgO or Ag NPs showed minimal toxicity to normal human cells at effective concentrations ²¹. Selectivity Index (SI) calculations, based on IC50 values for HDF cells vs. P. falciparum, revealed the highest selectivity for the (30:70) formulation (SI=3.6 for 3D7 strain; 0.59 for K1), indicating better parasite specificity, especially for the chloroquine-sensitive strain. The other formulations showed lower SI values, highlighting the need for further optimization to enhance safety and efficacy.

The core novelty of this study lies in its evaluation of the antiplasmodial activity of *A. millefolium*-derived MgO NPs against both chloroquine-sensitive (3D7) and chloroquine-resistant (K1) strains of *Plasmodium falciparum*. Among the three tested formulations, the (30:70) extract-based MgO NPs exhibited the lowest IC₅₀ (0.17 *mg/ml*) against 3D7, comparable to chloroquine itself (Figure 8, Table 1). Against the K1 strain, the same formulation showed an IC₅₀ of 1.04 *mg/ml*, which, although higher, still indicates meaningful antiplasmodial activity. The lower efficacy against K1 may stem from parasite-specific resistance mechanisms that affect cellular uptake or detoxification of nanoparticles.

Mechanistically, the observed antiparasitic effects may be attributed to several interrelated factors. First, the small particle size of MgO NPs enhances their internalization into infected erythrocytes, where they may interact directly with the parasite. Second, MgO NPs are known to generate Reactive Oxygen Species (ROS), which can disrupt intracellular redox homeostasis, damage parasite membranes, or interfere with DNA replication. Studies on ZnO and Ag NPs have demonstrated similar effects on protozoan parasites, including Leishmania and Plasmodium spp. 22-27. Third, the surfacebound phytochemicals from A. millefolium may synergistically contribute to antiplasmodial activity through membrane disruption or enzyme inhibition. The specific contribution of each mechanism requires further biochemical investigation.

The present study's findings are consistent with previous studies on other green-synthesized metallic nanoparticles with antiparasitic properties. For example, Azadirachta indica-derived Ag NPs inhibited P. falciparum 3D7 and RKL9 strains with IC50 values of 8–11 $\mu g/ml^{28}$, while Euphorbia hirta-mediated Ag NPs showed an IC50 of $100 \mu g/ml^{29}$. Although the IC50 values in the present study are somewhat higher, the use of MgO—a metal oxide generally considered less toxic and more biocompatible than silver, may offer advantages in terms of safety, scalability, and regulatory approval.

Despite encouraging results, this study has limitations. It was restricted to *in vitro* models and did not assess pharmacokinetics, biodistribution, or detailed mechanistic pathways. Future work should involve *in vivo* validation, toxicity profiling, and mechanistic studies to unravel the molecular interactions between greensynthesized MgO NPs and *Plasmodium* parasites.

Conclusion

In this study, a novel green synthesis approach was introduced for MgO-NPs using *A. millefolium* extracts in varying aqueous—ethanol ratios and demonstrated their promising antiplasmodial activity against *P. falciparum*. Among the tested formulations, the 30:70 (DW:EtOH) extract produced MgO-NPs with the strongest activity against the chloroquine-sensitive 3D7 strain (IC₅₀ = $0.17 \, mg/ml$), comparable to that of chloroquine.

These findings highlight the potential of *A. mille-folium*-based MgO-NPs as eco-friendly and effective candidates for developing alternative antimalarial therapies, particularly in the face of increasing drug resistance. Nonetheless, limitations such as the lack of *in vivo* validation and XRD-based crystallinity analysis should be addressed in future work. Further studies should also explore the mechanism of action and the possible broader-spectrum antimicrobial properties of these nanoparticles.

Acknowledgement

We would like to express our gratitude to those who kindly facilitated this study, particularly Ms. Zahra Farzaneh for her technical assistance.

All parts of the current study were approved by Ethic Committee of Tehran University of Medical Sciences (Ethic ID: IR.TUMS.MEDICINE.REC.1402.650).

Funding: Research funding from Tehran University of Medical Sciences (Grant Number: 1402-4-99-6 9744) is gratefully acknowledged.

Conflict of Interest

No potential conflict of interest is reported by the authors.

References

- World Health Organization 2024, World Malaria Report 2023, https://www.who.int/teams/global-malaria-programme/reports/world-malaria-report-2023.
- Baruah UK, Gowthamarajan K, Vanka R, Karri V, Selvaraj K, Jojo GM. Malaria treatment using novel nano-based drug delivery systems. J Drug Target 2017;25(7): 567-81.
- Mbatha LS, Akinyelu J, Chukwuma CI, Mokoena MP, Kudanga T. Current Trends and Prospects for Application of Green Synthesized Metal Nanoparticles in Cancer and COVID-19 Therapies. Viruses 2023;15(3):741.
- Vitalini S, Beretta G, Iriti M, Orsenigo S, Basilico N, Dall'Acqua S, et al. Phenolic compounds from Achillea millefolium L. and their bioactivity. Acta Biochim Pol 2011;58(2):203-9.

- Murnigsih T, Subeki, Matsuura H, Takahashi K, Yamasaki M, Yamato O, et al. Evaluation of the inhibitory activities of the extracts of Indonesian traditional medicinal plants against Plasmodium falciparum and Babesia gibsoni. J Vet Med Sci 2005;67(8):829-31.
- N Hasson R. Antibacterial activity of water and alcoholic crude extract of flower Achillea millefolium. Rafidain J Sci 2011;22(5):11-20.
- Verma SK, Nisha K, Panda PK, Patel P, Kumari P, Mallick M, et al. Green synthesized MgO nanoparticles infer biocompatibility by reducing in vivo molecular nanotoxicity in embryonic zebrafish through arginine interaction elicited apoptosis. Sci Total Environ 2020;713:136521.
- 8. Abdallah Y, Ogunyemi SO, Abdelazez A, Zhang M, Hong X, Ibrahim E, et al. The green synthesis of MgO nanoflowers using Rosmarinus officinalis L.(Rosemary) and the antibacterial activities against Xanthomonas oryzae pv. oryzae. BioMed Res Int 2019;2019(1):5620989.
- Hirphaye BY, Bonka NB, Tura AM, Fanta GM. Biosynthesis of magnesium oxide nanoparticles using Hagenia abyssinica female flower aqueous extract for characterization and antibacterial activity. Applied Water Science 2023;13(9):175.
- Berechet MD, Manaila E, Stelescu MD, Craciun G. The composition of essential oils obtained from Achillea millefolium and Matricaria chamomilla L., originary from Romania. Rev Chim 2017;68:2787-95.
- 11. Talapko J, Škrlec I, Alebić T, Jukić M, Včev A. Malaria: The Past and the Present. Microorganisms. 2019;7(6): 179.
- 12. Andrade MV, Noronha K, Diniz BP, Guedes G, Carvalho LR, Silva VA, et al. The economic burden of malaria: a systematic review. Malar J 2022;21(1):283.
- Mohammadi L, Pal K, Bilal M, Rahdar A, Fytianos G, Kyzas GZ. Green nanoparticles to treat patients with Malaria disease: An overview. Journal of Molecular Structure 2021;1229:129857.
- Kumar PP, Bhatlu ML, Sukanya K, Karthikeyan S, Jayan N. Synthesis of magnesium oxide nanoparticle by eco friendly method (green synthesis)—A review. Materials Today: Proceedings. 2021 Jan 1;37:3028-30.
- 15. Ogunyemi SO, Zhang F, Abdallah Y, Zhang M, Wang Y, Sun G, et al. Biosynthesis and characterization of magnesium oxide and manganese dioxide nanoparticles using Matricaria chamomilla L. extract and its inhibitory effect on Acidovorax oryzae strain RS-2. Artif Cells Nanomed Biotechnol 2019;47(1):2230-9.
- Palanisamy G, Pazhanivel T. Green synthesis of MgO nanoparticles for antibacterial activity. Int Res J Eng Technol. 2017 Aug 4;4(9):137-41.
- 17. Rotti RB, Sunitha DV, Manjunath R, Roy A, Mayegowda SB, Gnanaprakash AP, et al. Green synthesis of MgO nanoparticles and its antibacterial properties. Front Chem 2023;11:1143614.
- 18. Fatiqin A, Amrulloh H, Simanjuntak W. Green synthesis of MgO nanoparticles using Moringa oleifera leaf aqueous extract for antibacterial activity. Bulletin of the Chemical Society of Ethiopia 2021;35(1):161-70.

- Jeevanandam J, San Chan Y, Danquah MK. Biosynthesis and characterization of MgO nanoparticles from plant extracts via induced molecular nucleation. New Journal of Chemistry 2017;41(7):2800-14.
- 20. Kojom Foko LP, Eya'ane Meva F, Eboumbou Moukoko CE, Ntoumba AA, Ngaha Njila MI, Belle Ebanda Kedi P, et al. A systematic review on anti-malarial drug discovery and antiplasmodial potential of green synthesis mediated metal nanoparticles: overview, challenges and future perspectives. Malar J 2019;18(1):337.
- Khan AU, Khan M, Khan AA, Parveen A, Ansari S, Alam M. Effect of Phyto-Assisted Synthesis of Magnesium Oxide Nanoparticles (MgO-NPs) on Bacteria and the Root-Knot Nematode. Bioinorg Chem Appl 2022; 3973841.
- Gatou MA, Bovali N, Lagopati N, Pavlatou EA. MgO Nanoparticles as a Promising Photocatalyst towards

- 26. Shaba P, Pandey N, Sharma O, Rao J, Mishra A, Singh R. Screening of Achillea millefolium .L (Yarrow) flowers for its antitrypanosomal activity.
- 27. Barati A, Huseynzade A, Imamova N, Shikhaliyeva I, Keles S, Alakbarli J, et al. Nanotechnology and malaria: Evaluation of efficacy and toxicity of green nanoparticles and future perspectives. J Vector Borne Dis 2024;61(3): 340-56.
- Panneerselvam C, Murugan K, Amerasan D. Biosynthesis of silver nanoparticles using plant extract and its anti-plasmodial property. Advanced Materials Research 2015; 1086:11-30.
- Moraes-de-Souza I, de Moraes BPT, Silva AR, Ferrarini SR, Gonçalves-de-Albuquerque CF. Tiny Green Army: Fighting Malaria with Plants and Nanotechnology. Pharmaceutics 2024;16(6):699.

- Rhodamine B and Rhodamine 6G Degradation. Molecules 2024;29(18):4299.
- 23. Hanna DH, El-Mazaly MH, Mohamed RR. Synthesis of biodegradable antimicrobial pH-sensitive silver nanocomposites reliant on chitosan and carrageenan derivatives for 5-fluorouracil drug delivery toward HCT116 cancer cells. Int J Biol Macromol 2023;231:123364.
- Parthiban E, Manivannan N, Ramanibai R, Mathivanan N. Green synthesis of silvernanoparticles from Annona reticulata leaves aqueous extract and its mosquito larvicidal and antimicrobial activity on human pathogens. Biotechnol Rep (Amst) 2019;21:e00297.
- Santos AO, Santin AC, Yamaguchi MU, Cortez LE, Ueda-Nakamura T, Dias-Filho BP, et al. Antileishmanial activity of an essential oil from the leaves and flowers of Achillea millefolium. Ann Trop Med Parasitol 2010;104 (6):475-83.